

# Delayed separation in eastward, rotating flow on a $\beta$ -plane

By M. R. FOSTER

Department of Aeronautical and Astronautical Engineering, The Ohio State University

(Received 13 April 1984 and in revised form 26 November 1984)

We consider the small-Rossby-number flow of a fluid past an obstacle in a coordinate frame in which the rotation rate varies linearly in the direction normal to the flow in a manner that models the variation of the Coriolis force for midlatitude planetary motions. The eastward flow is characterized by strong upstream divergence of the streamlines like that noted by Davies & Boyer (1982), and a similarly severe streamline convergence in the lee of the obstacle. Such a structure occurs for small values of the  $\beta$ -parameter that measures the importance of the lateral angular-velocity variation. In this parameter range, Rossby waves occur, but are confined to a narrow region in the lee of the object. The presence of these waves modifies the edge velocity 'seen' by the Stewartson quarter layer in such a way as to delay the onset of separation beyond what one might expect based on the analysis of Walker & Stewartson (1974) for a flow without beta-effect.

---

## 1. Introduction

The flow of a rotating fluid past an obstacle generates a variety of interesting phenomena (see McCartney (1975) for a summary of the theoretical work to that date) including Taylor columns, inertial waves, and wakes that may, in some parameter ranges, include vortical structures. In such a flow, as in the case of a non-rotating fluid, separation of the boundary layer(s) on the surface of the object, when such layers exist, is likely to be the origin of the vorticity in such a wake. A first step toward understanding such features is the investigation of the separation phenomenon as it occurs in such a flow.

Walker & Stewartson (1972, 1974) and Crissali & Walker (1976) investigated the nature of separation for flow past an object in a uniformly rotating frame; in that case a point of zero skin friction occurs in the  $\frac{1}{4}$ -layer that bounds the Taylor column associated with the object. They found that the problem is mathematically identical with a certain MHD problem studied in detail by Leibovich (1967) and Buckmaster (1969). Walker & Stewartson (1974) found, for a fluid layer of depth  $h$  flowing past a hemisphere of radius  $ah$ , that separation will occur whenever the Rossby number  $Ro = U/\Omega h$  is larger than  $aE^{\frac{1}{2}}$ , where  $E = \nu/\Omega h^2$  is the Ekman number. Recently Page (1982) has investigated the separation of the inner-wall boundary layer for flow over shallow ( $O(E^{\frac{1}{2}})$ ) topography in a rotating cylindrical annulus. He found that, for any value of  $Ro/E^{\frac{1}{2}}$ , there is a maximum obstacle slope – for a sinusoidal shape,  $1.8E^{\frac{1}{2}}$  – below which no boundary-layer separation can occur. For larger values of the slope, the Rossby number must be smaller, in units of  $E^{\frac{1}{2}}$ , to avoid separation.

The only analysis, to this author's knowledge, on separation criteria for an object on a  $\beta$ -plane is that of Merkin (1980), in whose study  $\beta$  is  $O(1)$  and  $Ro \gg E^{\frac{1}{2}}$ ; we will

investigate flow at lower speeds, and shall find, as Merkin did, and also White (1971) in an experimental context, that the  $\beta$ -effect inhibits separation.

The work reported here began as a result of informal discussions the author was privileged to have during the summer of 1981 with Drs Davies and Boyer in regard to some of their observations (Davies & Boyer 1982). The experiments, conducted at the University of Wyoming in a rotating water channel, indicate that, in part of the parameter ranges studied, eastward flow past an obstacle on a  $\beta$ -plane is characterized by a spreading of the streamlines upstream of the obstacle, and a marked convergence of those streamlines immediately downstream of the cylindrical obstacle (see e.g. Davies & Boyer 1982, figures 5 and 6).

In this paper, we restrict the parameters for eastward flow past a short cylinder between parallel planes (cf. figure 1) by requiring that  $E^{\frac{1}{2}} \ll \beta \ll E^{\frac{1}{3}}$ . In §2 the consequences for the outer flow are shown to be a large upstream wake, bounded by free shear layers parallel to the oncoming flow and extending from one plane to the other (cf. figures 2 and 3 and §3). All of this structure is essentially two-dimensional, and independent of the cylinder height  $ad$ . The free shear layers meet the cylinder (and its upward extension to the top plane – the Taylor column) at its lateral extremes (the ‘shoulders’), carrying large amounts of fluid, which flow round the backside of the cylindrical column in a narrow rotational layer. The fluid flows out of the layer and into the inviscid region. This layer contains Rossby waves, and is discussed in detail in §4.

The fluid in this Rossby layer slips over the column (including that portion of the column coincident with the solid cylinder), and hence a Stewartson  $\frac{1}{4}$ -layer is required to satisfy the no-slip condition. In non- $\beta$ -plane flow, Walker & Stewartson (1972, 1974) found that the  $\frac{1}{4}$ -layer is nonlinear for  $Ro = O(E^{\frac{1}{2}})$ . In §5 the  $\frac{1}{4}$ -layer analysis shows that the layer becomes nonlinear for  $Ro = O(E/\beta)$ . Since  $E/\beta \ll E^{\frac{1}{2}}$  here, the nonlinearity occurs at a lower speed on the  $\beta$ -plane. Walker & Stewartson found separation occurring above a particular value of  $Ro/E^{\frac{1}{2}}$ , so we might expect a similar criterion for  $Ro\beta/E$ . Numerical integration of the nonlinear  $\frac{1}{4}$ -layer equation (cf. §6) shows that no point of zero wall shear develops. The structure of the Rossby layer above the  $\frac{1}{4}$ -layer is such as to inhibit separation. Apparently, then, separation is delayed to Rossby numbers much larger than  $E/\beta$ .

In §§6 and 7 we give details of the flow near the shoulders and at the rear stagnation point on the column.

If the flow past the cylinder is westward instead of eastward as required in this discussion, the analysis of §§2 and 3 goes through essentially unchanged. The Rossby layer and  $\frac{1}{4}$ -layer solutions in §§4 and 5, however, while correct for very small Rossby numbers, present some real difficulties for finite values of  $Ro$ , in particular  $O(E/\beta)$ . Resolution of this matter must await further work.

## 2. Formulation: outer expansion

Consider a homogeneous fluid confined between parallel planes, whose normals are aligned with the  $z$ -axis, about which the container rotates at angular velocity that varies with the  $y$ -direction as  $\Omega(1 + \beta y)$ . An object, on the lower of the two planes, disturbs the flow, which has uniform speed  $U$  far upstream,  $x = -\infty$  (see figure 1). In this rotating frame the dimensionless Navier–Stokes equations are

$$\nabla \cdot \mathbf{u} = 0, \quad (2.1)$$

$$Ro(\mathbf{u} \cdot \nabla) \mathbf{u} + 2(1 + \beta y) \mathbf{k} \times \mathbf{u} + \nabla p = E \nabla^2 \mathbf{u}. \quad (2.2)$$

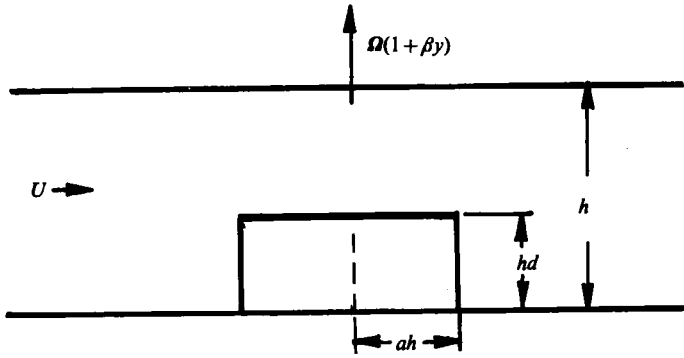


FIGURE 1. Geometric configuration for flow past a cylinder.

The  $y$ -variation in the rotation rate models, of course, such variations in midlatitude planetary flows, and is the ' $\beta$ -plane approximation' (cf. Holton 1979, p. 129 ff.). In the laboratory, such effects may be achieved, as is well known, by slightly tilting the upper of two bounding planes in a water channel. The equations of motion for such an arrangement may then be transformed into those above, in a new set of coordinates in which the two bounding planes are parallel, with the angular velocity of the frame of reference divided by  $1 - \beta y$ . The terms neglected in (2.2), resulting from the transformation, are  $O(\beta^2)$ ,  $O(Ro\beta)$  and  $O(E\beta)$ , which are all negligible if  $\beta$  is small.

We require, of course, that  $\mathbf{u} = \mathbf{0}$  on solid surfaces, and, for  $|x| \rightarrow \infty$ ,  $\mathbf{u} \rightarrow \mathbf{i}$ . (The velocities have been made non-dimensional with  $U$ , lengths with  $h$ .) We now restrict  $\beta$  in the following way:

$$1 \gg \beta \gg E^{\frac{1}{2}}, Ro. \tag{2.3}$$

We proceed with the outer expansion by writing

$$\mathbf{u} = \mathbf{u}_0 + \epsilon \mathbf{u}_1 + \dots, \tag{2.4}$$

$$p = p_0 + \epsilon p_1 + \dots, \tag{2.5}$$

where  $\text{ord}(\epsilon)$  is not yet determined. We know that, at  $z = 0$  and  $z = 1$ , the outer solutions must satisfy the Ekman compatibility conditions (cf. e.g. Foster 1972)

$$w = \pm \frac{1}{2} E^{\frac{1}{2}} \left( \frac{\partial v}{\partial x} - \frac{\partial u}{\partial y} \right) \quad \text{on } z = \begin{cases} 0 \\ 1 \end{cases}. \tag{2.6}$$

The expansions (2.4) and (2.5) must be inserted into (2.1), (2.2) and (2.6). Whatever the relative orders of  $Ro$ ,  $E$  and  $\beta$ , the leading-order result is

$$2\mathbf{k} \times \mathbf{u}_0 + \nabla p_0 = \mathbf{0},$$

$$\nabla \cdot \mathbf{u}_0 = 0.$$

To next order, quite distinct force balances may occur depending on the relative orders of the three small parameters. The most instructive way to see that is to write the  $(\ )_1$  vorticity equation:

$$Ro(\mathbf{u}_0 \cdot \nabla) \zeta_0 - 2 \frac{\partial w_1}{\partial z} \epsilon + 2\beta v_0 = 0, \tag{2.7}$$

$$\zeta_0 = \frac{\partial v_0}{\partial x} - \frac{\partial u_0}{\partial y}.$$

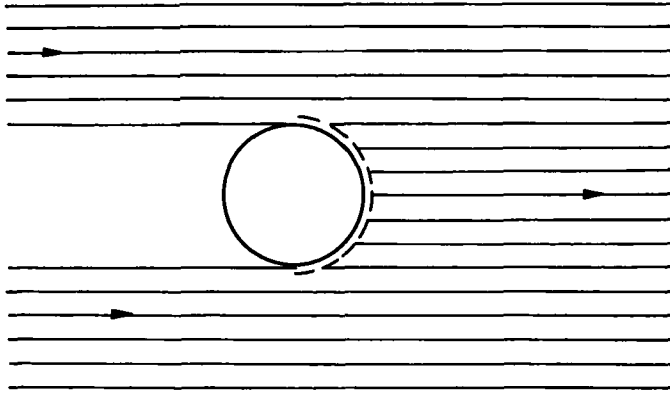


FIGURE 2. Outer flow solution.

Note that, from (2.6),  $\epsilon w_1$  is  $O(E^{\frac{1}{2}})$ ; if only  $\beta \gg E^{\frac{1}{2}}$  but  $Ro = O(\beta)$  one obtains the usual equation for Rossby waves; so, then, Rossby waves fill the inviscid flow. However, if  $Ro \ll \beta$ , and since  $\epsilon w_1$  is still  $O(E^{\frac{1}{2}})$ , under our condition (2.6), we obtain

$$v_0 = 0. \quad (2.8)$$

Thus, away from any thin viscous layers, there can be *no lateral motion*. All streamlines, then, in the outer flow are straight lines aligned with the upstream flow. Those lines lying in the range  $|y| < y_{\max}$ , where  $y_{\max}$  is the maximum half-width of the obstacle, intersect the object on its windward side; also, lines from the leeside of the obstacle penetrate the fluid to downstream infinity. Clearly fluid cannot flow into or originate from the solid boundary of the obstacle, so there must be thin boundary layers on the obstacle.

We now specify the obstacle as a circular cylinder of radius  $a$  and height  $d$ . It turns out, as we shall see in §4, that there can be no boundary layer to accommodate a large mass-flow rate on the upstream side of the cylinder, but one may exist on the leeside – actually on the entire circumscribing cylinder of the obstacle. The only recourse, then, is that, since  $\partial u_0 / \partial x$  is zero by continuity,  $u_0 = 0$  immediately ahead of the cylinder. Therefore we have

$$v_0 = w_0 = 0, \quad (2.9)$$

$$u_0 = \begin{cases} 1 & \text{for all } x > 0 \text{ and for } |y| > a, x < 0, \\ 0 & \text{for } x < 0 \text{ and } |y| < a. \end{cases} \quad (2.10)$$

Figure 2 shows the streamlines for this flow. Clearly the discontinuities at  $|y| = a$ ,  $x < 0$ , and the intersection of the streamlines with the leeside of the cylinder now require us to construct solutions in thin viscous regions to smooth the discontinuities. That is the subject of §§3–7.

### 3. Shear layers

We have seen that the outer solution constructed in §2 is discontinuous on  $|y| = a$ . This discontinuity is smoothed, of course, by retaining some of the terms ignored in obtaining (2.9). Writing  $y - a = (E^{\frac{1}{2}}/\beta)^{\frac{1}{2}} \hat{y}$  and substituting into (2.1) and (2.2) leads to the equation

$$\frac{\partial^2 \psi}{\partial \hat{y}^2} + \frac{\partial \psi}{\partial x} = 0. \quad (3.1)$$

Here  $\psi$  is the stream function, so

$$\hat{u} = \frac{\partial \psi}{\partial \hat{y}}, \quad v = -\frac{\partial \psi}{\partial x},$$

where  $\hat{u} = (E^{1/2}/\beta)^{1/2} u$  is a scaled velocity component. This layer represents a balance between the stretching of vortex lines by Ekman pumping and the lateral convection of the  $y$ -varying frame vorticity. No lateral viscous forces are important in the layer.

Far upstream, the volumetric flow rate in  $|y| < a$  is  $2a$ ; at the obstacle, because of the result (2.9), the flow rate is zero. What happens is that an amount of fluid  $a$  enters each thin shear layer on  $|y| = a$  at large negative  $x$  and flows into a sink at either  $y = a$  or  $y = -a$  and  $x = 0$ . It is this flow that is responsible for the leading-order solution to (3.1). Hence we write

$$\psi = \psi_0 + E^{1/2} \beta^{-1/2} \psi_1 + \dots \quad (3.2)$$

and substitute into (3.1); then both  $\psi_0$  and  $\psi_1$  satisfy (3.1) subject to the boundary conditions

$$\psi_0 = aH(\hat{y}) \quad \text{on } x = 0, \quad (3.3)$$

$$\psi_1 = \hat{y}H(\hat{y}) \quad \text{on } x = 0, \quad (3.4)$$

where  $H(x)$  is the Heaviside function. The  $\psi_0$  term involves the large mass flow mentioned above and  $\psi_1$  smooths the  $u_0$  discontinuity from (2.10). The solution is easily accomplished by Laplace transformation, and is

$$\psi_0 = a \left[ 1 - \frac{1}{2} \operatorname{erfc} \left( \frac{\hat{y}}{2(-x)^{1/2}} \right) \right], \quad (3.5)$$

$$\psi_1 = \hat{y}H(\hat{y}) + \left( \frac{-x}{\pi} \right)^{1/2} \exp \left( \frac{\hat{y}^2}{4x} \right) - \frac{1}{2} |\hat{y}| \operatorname{erfc} \left( \frac{|\hat{y}|}{2(-x)^{1/2}} \right). \quad (3.6)$$

Clearly both of these solutions have the property that they spread in the upstream directions; they are not uniformly valid to  $x = -\infty$ . Notice, however, that (3.1) contains (2.8). Therefore (3.1) may be solved in all of  $x < 0$  by writing  $x = (\beta/E^{1/2})X$ . Then  $\psi$  satisfies (3.1) with  $\hat{y}$  replaced by  $y$  and  $x$  by  $X$ . The boundary condition is at  $X = 0$  (for  $X = O(1)$ , the cylinder has infinitesimal  $X$ -direction width), where (3.2)–(3.4) combine to give

$$\psi = yH(y-a) \quad \text{on } X = 0 \text{ in } y > 0 \quad (3.7)$$

It may be shown using Laplace transforms that the solution for  $\psi$  is

$$\psi = -2 \left( \frac{-X}{\pi} \right)^{1/2} \sinh \left( \frac{ay}{2X} \right) \exp \left( \frac{a^2 + y^2}{4X} \right) + \frac{1}{2} y \left[ \operatorname{erfc} \left( \frac{a-y}{2(-X)^{1/2}} \right) + \operatorname{erfc} \left( \frac{a+y}{2(-X)^{1/2}} \right) \right]. \quad (3.8)$$

Figure 3 shows the streamlines in  $x < 0$  for a particular value of  $\beta/E^{1/2}$ . The shape of these lines is quite reminiscent of some of the photographs of Davies & Boyer (1982).

#### 4. The Rossby layer

It may easily be shown that the presence of the small  $\beta$ -term in (2.2) does not, to leading order, affect the presence of the usual Stewartson layers on the surface at  $r = a$ . The  $\frac{1}{2}$ - and  $\frac{1}{4}$ -layers smooth the discontinuities in tangential ( $v, w$ ) speeds at the boundary of the Taylor column. We discuss these layers in §5. What is different here is the fact that an  $O(1)$  volume flow enters the column at  $x = 0$ ,  $y = |a|$ , flows around the column boundary, and then downstream from the leeside of the cylinder. Such

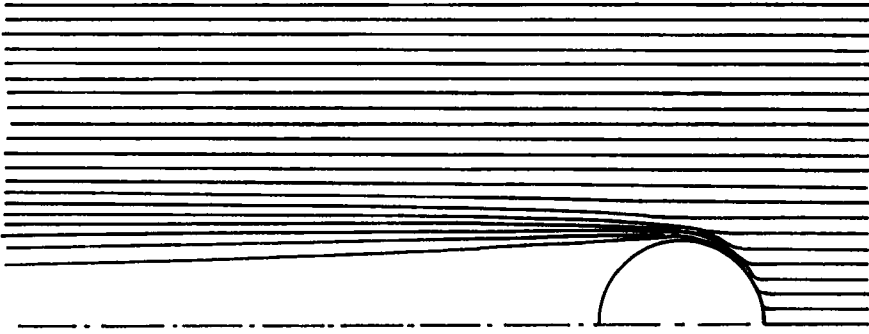


FIGURE 3. Streamlines for flow past a circular cylinder with  $E^{1/2}/\beta = 0.01$ , including the Rossby layer on the leeside of the cylinder.

a flow pattern is not consistent with the structure of either Stewartson layer, but is instead accomplished by what we may call a Rossby layer; it is a layer with the kind of force balance present in the shear layers described in §3, and it is a detrainng boundary layer.

Since this layer involves azimuthal motion along the cylinder, the azimuthal component of (2.2) is the dominant equation of interest here. Just as in conventional boundary-layer theory, the radial momentum equation indicates that there is no pressure change across the layer, so that the azimuthal pressure gradient from the external, inviscid flow, (2.9) and (2.10), is impressed on the fluid in the layer. Then, writing  $r-a = (E^{1/2}/\beta)\xi$ ,  $\psi' = -a\bar{\psi}$ , and, for the azimuthal velocity component,  $v = a(\beta/E^{1/2})\bar{v}$ , and substituting into the azimuthal component of (2.2), we obtain, on letting  $E \rightarrow 0$  and  $\beta \rightarrow 0$ ,

$$\lambda \left( u \frac{\partial \bar{v}}{\partial \xi} + \bar{v} \frac{\partial \bar{v}}{\partial \theta} \right) + \bar{v} + \bar{\psi} \cos \theta = -\frac{1}{2} \sin 2\theta, \quad (4.1)$$

where  $\lambda$  is the group of parameters  $Ro\beta/2E$ , which measures the importance of the nonlinear effects in the layer. Note too that  $(u, v)$  are now (and not as in §§2 and 3) radial and azimuthal velocity components, as they shall be throughout the remainder of the paper;  $\theta$  is the standard polar angle, with  $\theta = 0$  along the downstream  $x$ -axis. As mentioned in §1, we now suppose that  $Ro = O(E/\beta)$ , so that  $\lambda$  is  $O(1)$ . Equation (2.1) is satisfied by

$$u = -\frac{\partial \bar{\psi}}{\partial \theta}, \quad \bar{v} = \frac{\partial \bar{\psi}}{\partial \xi}. \quad (4.2)$$

The boundary conditions are no flow through the surface, and matching to (2.9) and (2.10), viz

$$\bar{\psi} = 0 \quad \text{on } \xi = 0, \quad \bar{v} = 0 \quad \text{on } \theta = \frac{1}{2}\pi, \quad (4.3)$$

$$\bar{\psi} \rightarrow -\sin \theta \quad \text{for } \xi \rightarrow \infty. \quad (4.4)$$

Remarkably, (4.1), on  $\xi = 0$ , reduces to a relatively simple, and in principle integrable, equation:

$$\lambda \bar{v} \frac{\partial \bar{v}}{\partial \theta} + \bar{v} + \frac{1}{2} \sin 2\theta = 0. \quad (4.5)$$

Solution of (4.1)–(4.5) is easy for  $\lambda = 0$ , namely

$$\bar{\psi} = -[1 - \exp(-\xi \cos \theta)] \sin \theta. \quad (4.6)$$

However, for any  $\lambda \neq 0$  the solution is complex indeed, as we shall see below.

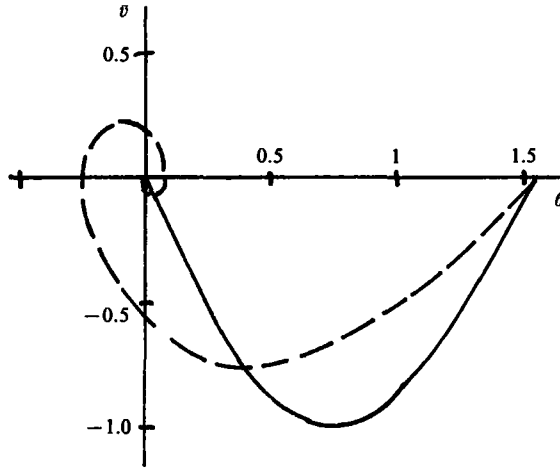


FIGURE 4.  $\psi = 0$  streamline in the Rossby layer for  $\lambda = 0.025$  (—) and  $1.0$  (-----).

Examination of the solutions of (4.5) may be most easily done in a  $(\bar{v}, \theta)$ -space. (This is actually a phase-plane for the Lagrangian coordinate  $\theta$ .) We show in figure 4 (the solid line) the nature of the solution for  $\lambda \leq \frac{1}{4}$ ; the solution trajectory proceeds from  $\theta = \frac{1}{2}\pi$  to  $\theta = 0$ . The singularity at  $\frac{1}{2}\pi$  is a saddle point; the singularity at 0 is a stable node. For the dashed line in figure 4,  $\lambda \geq \frac{1}{4}$ , and, though the first singularity is still a saddle point, the one at the origin has become a stable spiral:  $\bar{v}$  oscillates about  $\bar{v} = 0$ , and the trajectory actually passes beyond  $\theta = 0$ ! This phenomenon signals the onset of Rossby waves in the boundary layer.

Actually, a similar analysis may be performed for other streamlines. If we regard  $\bar{v}$  as a function of  $\theta$  and  $\bar{\psi}$ , then (4.1) becomes simply

$$\frac{\partial \bar{v}}{\partial \theta} = -\frac{\bar{v} + (\bar{\psi} + \sin \theta) \cos \theta}{\lambda \bar{v}}. \tag{4.7}$$

For the half of the Rossby layer in the first quadrant,  $\bar{\psi} < 0$ , so there is a singularity at  $\theta = -\sin^{-1} \bar{\psi}$ . So long as  $\lambda \leq \frac{1}{4}$  the singularity is a stable node as above; but, as above, when  $\lambda$  is larger than  $\frac{1}{4}$  the singularity may be a stable spiral or a node (cf. figure 5). In the vicinity of  $-\sin^{-1} \bar{\psi}$ , (4.7) has the approximate solution

$$v = K(\theta - \theta_0),$$

where

$$K = [-1 \pm (1 - 4\lambda \cos^2 \theta_0)^{\frac{1}{2}}] / 2\lambda$$

and  $\theta_0 = -\sin^{-1} \bar{\psi}$ . So streamlines oscillate about  $\theta_0 = -\sin^{-1} \bar{\psi}$  provided that  $\cos^2 \theta_0 > (4\lambda)^{-1}$ . If one writes (4.7) in terms of a Lagrangian variable  $\theta$ , (4.7) becomes the equation of a damped oscillator with a nonlinear spring;  $\lambda = \frac{1}{4}$  is 'critical damping' for the system.

An important thing to note in the phase trajectories of figure 5(b) is that they intersect  $\theta = \theta_0$  many times for  $\lambda \geq \frac{1}{4}$  if  $\theta < \cos^{-1} [(4\lambda)^{-\frac{1}{2}}]$ . Since  $\theta = 0$  is a line of symmetry for the flow, these streamlines also may intersect other lines from  $\theta < 0$  at  $\theta = 0$ , for  $\lambda \geq \frac{1}{4}$ . That is, in fact, impossible, however, and the only resolution is that there must be a square region of dimension  $E^{\frac{1}{2}}/\beta$  that turns the flow around near  $\theta = 0$  (cf. figure 6); in figure 5(b), that implies moving vertically along the  $\theta$ -axis from the point of intersection in  $\bar{v} < 0$  to a point of intersection in  $\bar{v} > 0$ , and then using the next leg of the same trajectory in  $\bar{v} > 0$ . For the case shown in figure 5(b),  $\lambda = 0.5$ ,

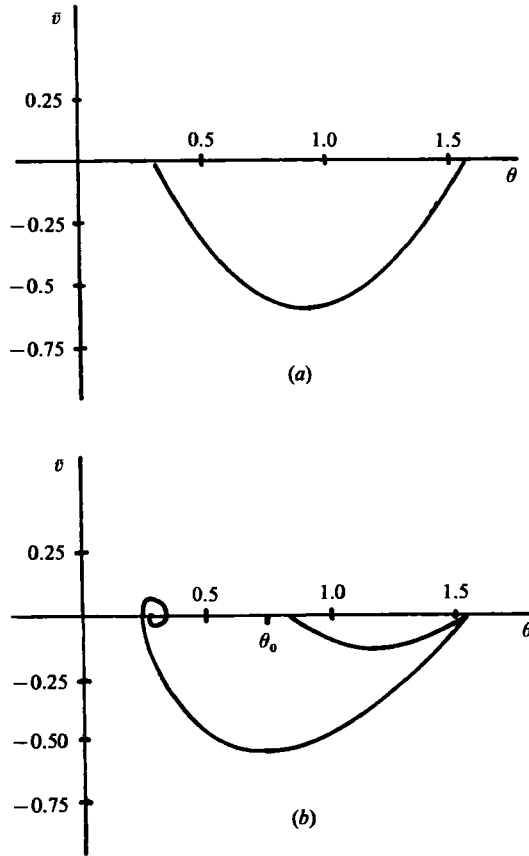


FIGURE 5. Streamlines in a  $(\bar{v}, \theta)$ -plane: (a)  $\bar{\psi} = -0.3$  for  $\lambda = 0.025$ ; (b)  $\bar{\psi} = -0.3$  and  $-0.75$  for  $\lambda = 0.5$ .

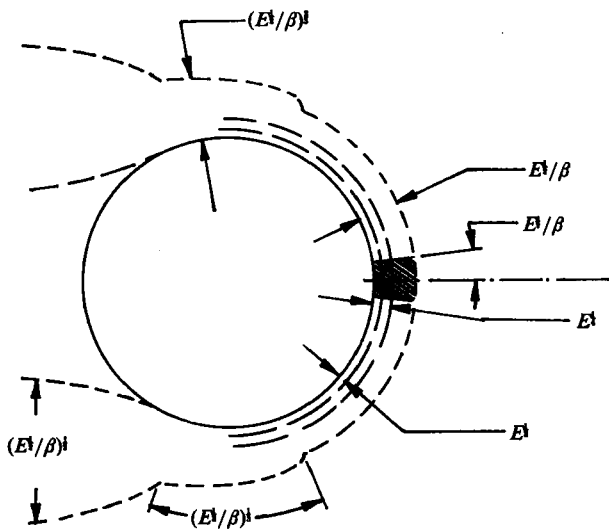
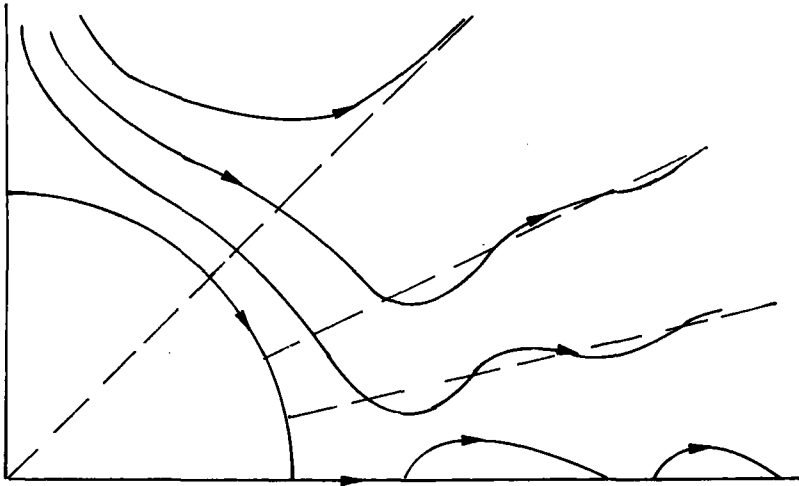


FIGURE 6. Diagram of the boundary- and shear-layer structure near the circular cylinder.




 FIGURE 7. Configuration of Rossby-layer streamlines for  $\lambda = \frac{1}{2}$ .

the value of  $\theta_0$  is  $\frac{1}{4}\pi$  and is noted on the graph. All trajectories terminating to the left of  $\theta_0$  do so in a spiral, and those to the right in a node. If one is to construct streamlines in physical space from these solutions in the  $(\bar{v}, \theta)$ -plane then solution of

$$\frac{\partial \xi}{\partial \bar{\psi}} = \frac{1}{\bar{v}} \quad (4.8)$$

is required. We show, in figure 7, schematic representations of typical streamlines under such an inversion, utilizing the ideas given above. To date, no detailed numerical solutions have been constructed for  $\lambda \geq \frac{1}{4}$ ; the numerical solution of (4.7) is easy enough, but the repeated crossings of  $\theta = \text{constant}$  lines by the *same* streamline make numerical implementation of (4.8) a nightmare. The appearance of the spiral singularities noted above is responsible, of course, for the wavelike streamline shape, and also the presence in the solution of a string of closed eddies on the line of symmetry,  $\theta = 0$ .

It has been possible to construct numerical solutions of (4.5), of course. If  $\bar{v}_i$  is the solution at  $\theta_i$ , with  $i = 1$  at  $\theta = \frac{1}{2}\pi$ , central differencing of (4.5) leads a nonlinear difference equation whose exact solution is

$$\bar{v}_i = \frac{h}{2\lambda} - q^{\frac{1}{2}},$$

where

$$q = \left(\frac{h}{2\lambda}\right)^2 + \frac{\bar{v}_{i-1}^2}{\lambda} + \frac{h}{2\lambda} (\sin 2\theta_i + \sin 2\theta_{i-1}) + \frac{h}{\lambda} \bar{v}_{i-1}.$$

We show, in figure 8, solutions of this equation for typical values of  $\lambda$  and for  $h = 0.0157$ , i.e. for 100 points between  $\theta = \frac{1}{2}\pi$  and 0.

Equation (4.1) also has a similarity solution near  $\theta = \frac{1}{2}\pi$ . If we write  $\bar{\psi} = F(l)$ , where  $l = (\frac{1}{2}\pi - \theta)\xi$ , substitution into (4.1) gives the following ordinary differential equation for  $F$ :

$$\lambda(F')^2 - F' - F - 1 = 0, \quad (4.9)$$

$$F(0) = 0, \quad F(\infty) = -1.$$

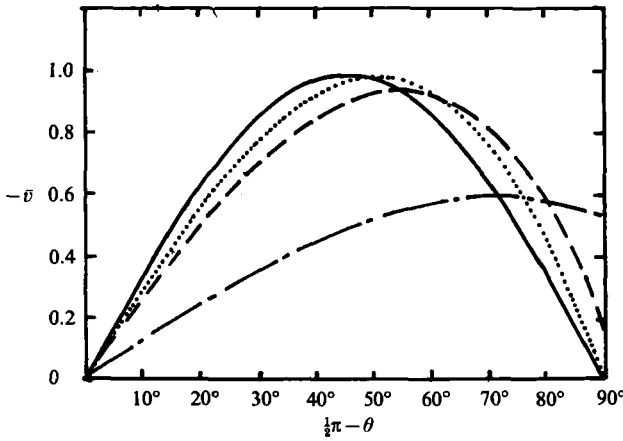


FIGURE 8. Surface speed in the Rossby layer for  $\lambda = 0.025$  (—),  $0.25$  (·····),  $0.5$  (-----) and  $5$  (-·-·-·).

The solution is easily found to be

$$F = -1 + \frac{S^2 - 1}{4\lambda}, \tag{4.10}$$

where  $S$  is given implicitly by

$$S - (1 + 4\lambda)^{\frac{1}{2}} + \log \left( \frac{S - 1}{(1 + 4\lambda)^{\frac{1}{2}} - 1} \right) = -l. \tag{4.11}$$

For  $\lambda \downarrow 0$ ,  $S \rightarrow 1 + 2\lambda \exp(-l)$  from (4.11), and so

$$F \rightarrow -1 + \exp(-l),$$

which agrees with (4.6).

The Rossby waves that occur here are the only Rossby waves present in the flow in this range of parameters; they are confined to this thin layer. Of course, as  $Ro$  increases above  $E\beta$ , the waves are convected downstream, out of the layer, and into the whole expanse of the fluid downstream of the cylinder.

Note too that the neglect of the nonlinear terms in the free-shear-layer equations of §3 requires that  $Ro$  be small compared with  $E^{\frac{1}{2}}/\beta^{\frac{1}{2}}$ . If  $\lambda = O(1)$  this simply leads to the requirement that  $\beta^{\frac{1}{2}}E^{\frac{1}{2}} \ll 1$ , which is obviously satisfied. In other words, the Rossby layer (and, as we shall see, the  $\frac{1}{4}$ -layer) becomes nonlinear before the shear layers at  $y = |a|$ . The linearity of the Ekman layer is also assured provided only that  $\beta \ll 1$ , so long as  $\lambda = O(1)$ .

### 5. Stewartson layers

As noted previously, on  $r = a$  there are the usual  $\frac{1}{4}$  and  $\frac{1}{3}$  Stewartson layers. Whether the cylinder has height 1 or  $d < 1$ , the structure of the  $\frac{1}{4}$ -layer is as though the cylinder were solid (Foster 1972). The outer, Rossby layer, whose thickness is  $E^{\frac{1}{2}}/\beta$ , is thicker than the  $E^{\frac{1}{2}}$  layer provided also that  $\beta \ll E^{\frac{1}{2}}$ . In combination with (2.3) and the discussion in §4, the complete parameter restriction is then

$$E^{\frac{1}{2}} \ll \beta \ll E^{\frac{1}{2}}, \quad Ro = O\left(\frac{E}{\beta}\right). \tag{5.1}$$

Were  $\beta$ , on the other hand, of order  $E^{\frac{1}{2}}$ , the Rossby layer and the  $\frac{1}{4}$ -layer would merge into a single viscous layer containing damped Rossby waves. We saw from §4 that the presence of the nonlinear term in the Rossby layer is valid for  $Ro$  as large as  $E/\beta$ , which is large compared with  $E^{\frac{1}{2}}$ . If  $\beta$  were as large as  $E^{\frac{1}{2}}$ ,  $Ro$  could be no more than  $O(E^{\frac{1}{2}})$ , so the nonlinearity enters at an even lower speed in that case.

*One-third layer*

The  $\frac{1}{3}$ -layer, the innermost of the two Stewartson layers (see figure 8), to lowest orders in the asymptotic expansion, is just the same as the  $\frac{1}{3}$ -layer discussed in Foster (1972). If we expand the azimuthal velocity, for example, in the usual way, we have

$$v = E^{-\frac{1}{3}}\beta(v_0 + E^{\frac{1}{3}}v_1 + E^{\frac{2}{3}}v_2 + \dots). \tag{5.2}$$

The  $E^{-\frac{1}{3}}\beta$  scale derives from the order of the azimuthal velocity in the Rossby layer of §4.  $w$  has a similar expansion, and definition of the usual  $\frac{1}{3}$ -layer variable  $\eta = (r-a)/E^{\frac{1}{3}}$  leads, on substitution into (2.1) and (2.2), to the familiar  $\frac{1}{3}$ -layer equations, with neglected terms  $O(E^{\frac{1}{3}})$ :

$$\frac{\partial^2 v}{\partial \eta^2} = -2 \frac{\partial w}{\partial z}, \quad \frac{\partial^3 w}{\partial \eta^3} = 2 \frac{\partial v}{\partial z}, \tag{5.3}$$

where the  $(v, w)$  stands for any term in the series. The expansion must be inserted into the Ekman conditions (2.6) to obtain the boundary conditions on  $z = 0, 1$ . That process leads to the following conditions:

$$w_0 = 0, \quad w_1 = 0 \quad \text{on } z = 0 \text{ and } z = 1. \tag{5.4}$$

Again  $(v_0, w_0)$  and  $(v_1, w_1)$  separately satisfy (5.3). In addition, the solutions must be matched to the  $\frac{1}{4}$ -layer solutions, which we denote by  $V$  and  $W$ . Those matching conditions are, for  $v$ ,

$$\left. \begin{aligned} v_0 &\rightarrow V(0 \pm) \quad \text{for } \eta \rightarrow \pm \infty, \\ v_1 &\rightarrow V'(0 \pm) \eta \quad \text{for } \eta \rightarrow \pm \infty. \end{aligned} \right\} \tag{5.5}$$

Solutions to (5.2)–(5.5) depend crucially on the nature of the singularities of the solutions of (5.3), as detailed by Moore & Saffman (1969); the analysis of a  $\frac{1}{3}$ -layer containing a  $270^\circ$  corner as we have here was given by Foster (1972). While not repeating that analysis here, suffice it to say that the  $(v_0, w_0)$  and  $(v_1, w_1)$  solutions are found to be regular. Use of a procedure used by Hocking (1967) shows that there is only one regular solution for  $(v_0, w_0)$  also satisfying the requirement that  $v_0 = 0$  on that part of  $\eta = 0$  on which  $z < d$ , viz  $w_0 = 0$  and  $v_0 = 0$ . Therefore we obtain from (5.5)

$$V(0+) = V(0-) = 0. \tag{5.6}$$

Since there is no interior flow over the bump ( $r < a, z > d$ ) there is therefore no  $\frac{1}{4}$ -layer on  $r = a -$  (cf. Foster 1972). We proceed now to a discussion of the flow in the  $\frac{1}{4}$ -layer.

*One-quarter layer*

The tangential velocity at  $\xi = 0$  in the Rossby layer must be brought to zero at  $r = a$  by the  $\frac{1}{4}$ -layer. So we write  $r - a = E^{\frac{1}{4}}Y$  for the  $\frac{1}{4}$ -layer coordinate,  $v = -(\beta/E^{\frac{1}{4}})V$  and  $u = (\beta/E^{\frac{1}{4}})U$ ; substitution into (2.1) and (2.2) gives

$$\left. \begin{aligned} \frac{\partial U}{\partial Y} + \frac{\partial V}{\partial s} &= 0, \\ 2a\lambda \left( U \frac{\partial U}{\partial Y} + V \frac{\partial V}{\partial s} \right) + 2(V - V_e) - 2a\lambda V_e \frac{dV_e}{ds} &= \frac{\partial^2 V}{\partial Y^2}, \end{aligned} \right\} \tag{5.7}$$

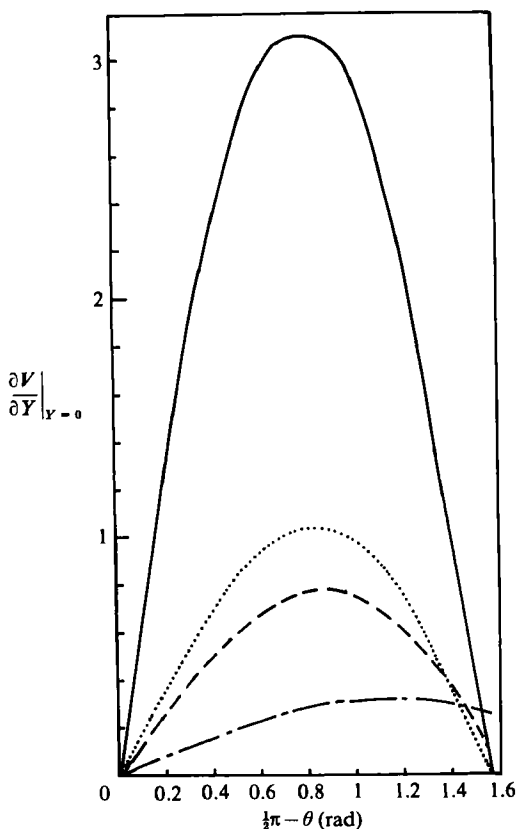


FIGURE 9. Surface stress in the  $\frac{1}{4}$ -layer solution for  $\lambda = 0.025$  (—), 0.25 (·····), 0.5 (-----) and 5 (-·-·-).

where  $s$  is a streamwise coordinate given by  $a(\frac{1}{2}\pi - \theta)$ . The boundary conditions require that this solution match the Rossby-layer solution of §4 as  $Y \rightarrow \infty$ . If we denote the solution of (4.5) evaluated on  $\xi = 0$  by  $V_e(s)$  then

$$V \rightarrow V_e \quad \text{as } Y \rightarrow \infty. \quad (5.8)$$

As we have just determined, the structure of the  $\frac{1}{3}$ -layer requires, from (5.6), that

$$V = 0 \quad \text{on } Y = 0. \quad (5.9)$$

For very small  $\lambda$ , (5.7) linearizes to the usual  $\frac{1}{4}$ -layer equation. The solution for  $\lambda = 0$ , corresponding to the linear Rossby-layer solution (4.6), is

$$V = \sin \theta \cos \theta (1 - \exp(-\sqrt{2} Y)). \quad (5.10)$$

Numerical solutions of (5.7), for  $\lambda$  not small, have been obtained by Buckmaster (1969) in a different context, for different boundary conditions, and related by Walker & Stewartson (1972) to the  $\frac{1}{4}$ -layer solution for flow past a circular cylinder (no  $\beta$ -effect). They found that the solution develops a point of zero shear stress, indicative apparently of separation, whenever  $\lambda$ , in our notation, is larger than  $\frac{1}{4}$ . That corresponds, in their case, to a particular ratio of  $Ro/E^{\frac{1}{2}}$ . Since, unlike the Walker & Stewartson problem,  $V_e$  itself is a function of  $\lambda$ , resulting as it does from the Rossby-layer structure, the calculation must be redone for each value of  $\lambda$ .

The numerical solutions reported here have been obtained by differencing (5.7) with central differences in the  $Y$ - and  $s$ -directions. Since no flow reversal occurs, there is no difficulty with the stability of the Crank–Nicholson algorithm owing to the convection terms. Figure 9 shows the result of the calculations in terms of shear at the wall,  $\partial V/\partial Y$  at  $Y = 0$ . In the numerical results reported here, the  $Y$ -step is 0.01, with 100 steps total, and the  $s$ -step is 0.001 963. The truncation error has been checked by reducing the step sizes by a factor of 2; the results are altered by no more than 0.44 % from  $\theta = \frac{1}{2}\pi$  to within  $2.8^\circ$  of  $\theta = 0$  for  $\lambda = 0.025$ ; at  $0.68^\circ$  the error is 2.0 %. Very close to the rear stagnation point, at  $\theta = 0.12^\circ$ , the errors are 17 %. So, except for a very small region near  $\theta = 0$ , the solutions given here are quite accurate. Note that a point of zero shear does occur at  $\theta = 0$  for all values of  $\lambda < \frac{1}{4}$ ; however, for larger  $\lambda$ -values, owing to the development of Rossby waves above the  $\frac{1}{4}$ -layer, the zero shear does *not* advance upward from  $\theta = 0$ ; in fact, the shear at  $\theta = 0$  becomes positive.

Thus we conclude that, unlike the situation that occurs for  $\beta = 0$ , the presence of an outer wavelike layer above the  $\frac{1}{4}$ -layer delays the onset of separation to higher Rossby numbers than those one might relate to the appearance of the nonlinear term in the shear-layer equations. Even though the speeds are very high in this  $\frac{1}{4}$ -layer, for all Rossby numbers of order  $E\beta^{-1}$  and smaller, no separation can occur.

In the  $\frac{1}{2}$ -layer segment above, the tacit assumption is that nonlinearities are not important. A careful evaluation of the orders of magnitude of the terms neglected in (5.3) shows the nonlinear term to be  $O(\lambda E^{\frac{1}{2}})$ , so that the  $E^{\frac{1}{2}}$  term in (5.2) will be first affected.

## 6. Shoulder region

All of the fluid that flows through the shear layers (§3) on  $y = \pm a$  flows into the Rossby layers at their beginnings at the shoulders of the cylinder (at  $\theta = \pm \frac{1}{2}\pi$ ). In this section we show that a region in the immediate vicinity of those shoulders facilitates the connection between those two singular layers. Figure 6 illustrates the scaling of this joining region, which accepts the fluid from upstream and turns it, to flow round the back of the cylinder.

A general investigation of all of the possible regions near  $\theta = \frac{1}{2}\pi$  and  $r = a$ , though it is for brevity not repeated here, shows that there is only one ‘distinguished limit’. That corresponds to writing the coordinates as  $r - a = \delta^2 \rho$  and  $\theta = \frac{1}{2}\pi - \delta \chi$ , where  $\delta = (E^{\frac{1}{2}}/\beta)^{\frac{1}{2}}$ . On substituting into (2.1) and (2.2), and eliminating the pressure, we obtain the vorticity equation for the stream function  $\bar{\psi} = -a\psi$  of §4:†

$$\lambda \frac{\partial}{\partial \rho} \left\{ \frac{\partial(\bar{\psi}, \partial\bar{\psi}/\partial\rho)}{\partial(\chi, \rho)} \right\} + \frac{\partial^2 \bar{\psi}}{\partial \rho^2} + \frac{1}{a} \frac{\partial \bar{\psi}}{\partial \chi} + \chi \frac{\partial \bar{\psi}}{\partial \rho} = 0. \quad (6.1)$$

The boundary condition on the solid surface is

$$\bar{\psi} = 0 \quad \text{on } \rho = 0. \quad (6.2)$$

Writing the solution in the Rossby layer in these coordinates and taking the limit  $\delta \rightarrow 0$  leads to the matching condition for  $\chi \rightarrow \infty$ :

$$\bar{\psi} \rightarrow \frac{S^2(\rho\chi) - 1}{4\lambda} - 1 \quad \text{for } \chi \rightarrow \infty. \quad (6.3)$$

† The author is grateful to a referee for pointing out difficulties in an earlier version of this equation, which then led to the proper analysis.

A similar procedure for the leading-order solution for the shear layer in §3 results in the matching condition for  $\chi$  large and negative, viz

$$\bar{\psi} \rightarrow -1 - \frac{1}{2} \operatorname{erfc} \left( \frac{\rho - \frac{1}{2} a \chi^2}{2(-a\chi)^{\frac{1}{2}}} \right) \quad \text{for } \chi \rightarrow -\infty. \quad (6.4)$$

Finally, for  $\rho \rightarrow \infty$  the solution must match to the outer solution, so

$$\psi \rightarrow -a \quad \text{for } \rho \rightarrow \infty. \quad (6.5)$$

For  $\chi \rightarrow -\infty$ , (6.1) has an asymptotic solution of the form

$$\bar{\psi} \sim A(\sigma) + \frac{1}{2} \lambda (-a\chi)^{-\frac{3}{2}} B(\sigma) + O((-a\chi)^{-\frac{5}{2}}), \quad \sigma = \frac{\rho - \frac{1}{2} a \chi^2}{2(-a\chi)^{\frac{1}{2}}}. \quad (6.6)$$

Substitution of (6.5) into (6.1), and considerable algebra, leads to a sequence of equations for  $A, B, \dots$ :

$$A'' + 2\sigma A' = 0, \quad (6.7)$$

$$C'' + 2\sigma C' + 4C = (A')^2, \quad B = \int_0^\sigma C(\bar{\sigma}) d\bar{\sigma}. \quad (6.8)$$

The solution of (6.7) that satisfies (6.2) and (6.5) is, of course,

$$A = -\left(1 - \frac{1}{2} \operatorname{erfc}(\sigma)\right), \quad (6.9)$$

which means, under the matching condition (6.4), that the (6.6) solution indeed matches to the shear layer for  $\chi \rightarrow -\infty$ , as required. The solution of (6.8) may be obtained by standard methods; suffice it to say here that, for

$$A \sim -\left(1 - \frac{1}{2\sigma\pi^{\frac{1}{2}}} e^{-\sigma^2}\right), \quad B \sim \text{const} \times \sigma^3 e^{-\sigma^2} \quad \text{for } \sigma \rightarrow \infty.$$

In similar fashion, an asymptotic solution to (6.1) for  $\chi \rightarrow \infty$  may be found:

$$\psi \sim R(\rho\chi) + \chi^{-3} T(\rho\chi) \quad \text{for } \chi \rightarrow \infty, \quad (6.10)$$

where substitution into (6.1) gives an equation for  $R$  that is identical with (4.9) for  $F(l)$ ;  $T(\tau)$  is a solution of the rather complicated equation

$$(1 + 3\lambda R') T'' + (1 - 2\lambda R') T' - 3\lambda R''' T = -\tau R'. \quad (6.11)$$

So, by the boundary conditions (6.2) and (6.5),  $R(\tau)$  is identical with  $F(l)$ . Some WKB-style analysis leads to the asymptotic solutions for  $R$  and  $T$ :

$$R(\tau) \sim -1 + \frac{(1+4\lambda)^{\frac{1}{2}} - 1}{2\lambda} e^{-\tau} \quad \text{for } \tau \rightarrow \infty, \quad (6.12)$$

$$T(\tau) \sim -\frac{(1+4\lambda)^{\frac{1}{2}} - 1}{2\lambda} \tau e^{-\tau} \quad \text{for } \tau \rightarrow \infty. \quad (6.13)$$

Hence we have demonstrated that solutions to (6.1) match to the Rossby layer for  $\chi \rightarrow \infty$ , using the expansion (6.10), and match to the shear layer for  $\chi \rightarrow -\infty$ , utilizing the expansion (6.6).

## 7. Rear stagnation point

Near the rear stagnation point on the cylindrical column that circumscribes the obstacle, §5 indicated that, for  $\lambda > \frac{1}{4}$ , the azimuthal velocity in the Rossby layer is

not zero. (For  $\lambda < \frac{1}{4}$ ,  $v \rightarrow 0$ , as  $\theta \rightarrow 0$ , so there is no difficulty.) The Rossby-layer scalings break down for  $\theta = O(E^{\frac{1}{2}}/\beta)$ , so to investigate this region of non-validity of the Rossby-layer equations we write  $r-a = (E^{\frac{1}{2}}/\beta)\xi$ , as in the Rossby layer, and  $\theta = (E^{\frac{1}{2}}/\beta)\bar{\theta}$ . Insertion into (2.2), elimination of the pressure, and use of the continuity equation to define the stream function as before, leads to the vorticity equation for  $\bar{\psi}$  in the region:

$$\lambda \frac{\partial(\bar{\psi}, \nabla_1^2 \bar{\psi})}{\partial(\bar{\theta}, \xi)} + \frac{E^{\frac{1}{2}}}{\beta} \left\{ \nabla_1^2 \bar{\psi} - \frac{\partial \bar{\psi}}{\partial \bar{\theta}} \right\} = 0, \quad (7.1)$$

where

$$\nabla_1^2 = \frac{\partial^2}{\partial \xi^2} + \frac{1}{a^2} \frac{\partial^2}{\partial \bar{\theta}^2}.$$

For  $\lambda = O(1)$  the proper limit of (7.1) for  $E \rightarrow 0$ , under (5.1), retains the first term only, whose solution is

$$\nabla_1^2 \bar{\psi} = G(\bar{\psi}). \quad (7.2)$$

Note that (7.2) is not the solution of (7.1) unless  $\lambda \gg E^{\frac{1}{2}}/\beta$ , which again is not a problem, since there is no need for such a region as this unless  $\lambda > \frac{1}{4}$ .

The boundary conditions are

$$\bar{\psi} = 0 \quad \text{on } \xi = 0, \bar{\theta} > 0 \text{ and on } \bar{\theta} = 0, \xi > 0. \quad (7.3)$$

In addition, the solution must match to the outer flow for  $\xi \rightarrow \infty$ , and to the Rossby-layer solution for  $\bar{\theta} \uparrow \infty$ . Thus

$$\begin{aligned} \bar{\psi} &\rightarrow 0 \quad \text{for } \xi \rightarrow \infty, \\ \bar{\psi} &\rightarrow \bar{\psi}_R(\xi, 0) \quad \text{for } \bar{\theta} \rightarrow \infty, \end{aligned} \quad (7.4)$$

where  $\bar{\psi}_R(\xi, \theta)$  denotes the Rossby-layer solution of §4. The form of the function  $\bar{\psi}_R(\xi, 0)$  determines the function  $G(\bar{\psi})$ . That means that the equation

$$\frac{d^2 \bar{\psi}_R}{d\xi^2}(\xi, 0) = G(\bar{\psi}_R(\xi, 0)) \quad (7.5)$$

must be inverted to obtain  $G(\bar{\psi})$ ; then the solution may proceed.

Solution of (7.2) under (7.3)–(7.5) is technically difficult, even for simple forms of  $\bar{\psi}_R(\xi, 0)$ . Since, as discussed in §4, there is no analytical or numerical solution available for the Rossby layer, the function  $\bar{\psi}_R(\xi, 0)$  is not known. However, the discussion there indicates a great deal of information about the form of the solution, if not the details. From figures 4, 5 and 7 it is clear that the quantity  $\bar{\psi}_R(\xi, 0)$  is oscillatory, the boundary conditions indicating that it vanishes on both  $\xi = 0$  and  $\xi = \infty$ , so there is no *net* flow into this region.

Some indication of the relative complexity of this turning region may be given by examining the asymptotic behaviour for  $\bar{\theta} \rightarrow \infty$ . Let  $\bar{\psi} = \bar{\psi}_R(\xi, 0) + \phi$ , where  $|\phi|$  should be arbitrarily small for  $\bar{\theta}$  sufficiently large. Substitution into (7.2) leads to the equation for  $\phi$ , viz

$$\nabla_1^2 \phi = f(\xi) \phi, \quad (7.6)$$

where we have written  $f(\xi)$  for  $G'(\bar{\psi}_R)$ . Actually, differentiation of (7.5) with respect to  $\xi$  gives  $f(\xi) = \bar{\psi}_R'''/\bar{\psi}_R'$ , which is more useful. Separation of variables in (7.6) gives the bounded solution

$$\phi = \int_0^\infty H(\xi, k) e^{-k\bar{\theta}} dk, \quad (7.7)$$

and  $H(\xi, k)$  is the solution of

$$H'' = \left( f(\xi) - \frac{k^2}{a^2} \right) H \quad (7.8)$$

(( ' ) denotes a  $\xi$ -derivative). Boundary conditions (7.3) and (7.4) give conditions on  $H$ :

$$H(0, k) = H(\infty, k) = 0. \quad (7.9)$$

Since we are interested in the solution for  $\bar{\theta} \rightarrow \infty$ , Watson's Lemma applied to (7.7) leads to the asymptotic form for  $\phi$ :

$$\phi \sim \frac{1}{\bar{\theta}} H(\xi, 0) \quad \text{for } \bar{\theta} \rightarrow \infty. \quad (7.10)$$

For  $H_0(\xi) \equiv H(\xi, 0)$ , (7.8) shows that

$$H_0'' = f(\xi) H_0. \quad (7.11)$$

Using (7.9) and integrating the product of (7.11) and  $H_0$ , we find that

$$\int_0^\infty (H_0')^2 d\xi + \int_0^\infty f(\xi) H_0^2 d\xi = 0, \quad (7.12)$$

from which we find a necessary condition for (7.10) to exist:

$$f < 0 \quad \text{for some values of } \xi < \infty. \quad (7.13)$$

Since  $f(\xi)$  is not known because of the difficulties of the Rossby-layer solution, we turn to examination of this solution behaviour when  $\xi$  is also large. Linearizing (4.1) for  $\xi \rightarrow \infty$  easily leads to the large- $\xi$  form of the solution on  $\theta = 0$ . It is

$$\bar{v}|_{\xi=0} = \frac{\partial \bar{\psi}_R}{\partial \xi}(\xi, 0) \sim \text{const} \times \cos(\omega\xi + \Phi) e^{-\xi/2\lambda}, \quad (7.14)$$

if  $\omega = \frac{1}{2}(4\lambda - 1)^{\frac{1}{2}}$  and  $\Phi$  is a phase-angle. Since  $f = \bar{\psi}_R''' / \bar{\psi}_R$ , (7.14) gives

$$f(\xi) \sim \frac{\frac{1}{2} - \lambda}{\lambda} + \frac{\omega}{\lambda} \tan(\omega\xi + \Phi). \quad (7.15)$$

Obviously (7.15) guarantees that the solvability condition (7.13) is satisfied.

Solution of (7.11) and (7.15) may be accomplished by WKB techniques (Bender & Orszag 1978); (7.11) has an infinite number of turning points, which are separated in  $\xi$ , for large  $\xi$  – from (7.15) – by  $\pi/\omega$ . The solution, which we do not write here, takes the form of exponentials and oscillations at each value of  $\xi$ , corresponding to right- or left-side of the turning points.

Thus an asymptotic solution to (7.2)–(7.5) that matches to the Rossby-layer solution appears to exist, although it is complicated.

In §5 we gave the structure of the  $\frac{1}{4}$ -layer, which takes the non-zero surface speed  $\bar{v}$  at the base of the Rossby layer to zero, in order to satisfy no-slip. Since  $E^{\frac{1}{2}}/\beta \gg E^{\frac{1}{2}}$ , an extension of that  $\frac{1}{4}$ -layer exists beneath this corner region. Since, by (7.3),  $\bar{v} \rightarrow 0$  as  $\theta \rightarrow 0$ , the  $\frac{1}{4}$ -layer will see a rapid decline in edge velocity, and may separate; however, since all of this occurs in a tiny region  $o(1)$  on the outer scales, if separation indeed occurs here, it provides insignificant consequences to the global flow structure.

The author is grateful to Professors Burggraf and Conlisk for several helpful discussions on this work. This material is based upon work supported by the National Science Foundation under Grant ATM-8212838.



## REFERENCES

- BENDER, C. M. & ORSZAG, S. A. 1978 *Advanced Mathematical Methods for Scientists and Engineers*. McGraw-Hill.
- BUCKMASTER, J. 1969 Separation and magnetohydrodynamics. *J. Fluid Mech.* **38**, 481.
- CRISSALI, A. J. & WALKER, J. D. A. 1976 Non-linear effects for the Taylor-column problem for a hemisphere. *Phys. Fluids* **19**, 1661.
- DAVIES, P. A. & BOYER, D. L. 1982 Flow past a circular cylinder on a  $\beta$ -plane. *Phil. Trans. R. Soc. Lond. A* **306**, 533.
- FOSTER, M. R. 1972 The flow caused by the differential rotation of a right circular cylindrical depression in one of two rapidly rotating parallel planes. *J. Fluid Mech.* **53**, 647.
- HOCKING, L. M. 1967 Boundary and shear layers in a curved rotating pipe. *J. Math. and Phys. Sci.* **1**, 123.
- HOLTON, J. R. 1979 *An Introduction to Dynamic Meteorology*. 2nd edn. Academic.
- LEIBOVICH, S. 1967 Magnetohydrodynamic flow at a rear stagnation point. *J. Fluid Mech.* **19**, 401.
- MCCARTNEY, M. S. 1975 Inertial Taylor columns on a beta plane. *J. Fluid Mech.* **68**, 71.
- MERKINE, L.-O. 1980 Flow separation on a  $\beta$ -plane. *J. Fluid Mech.* **99**, 399.
- PAGE, M. A. 1982 Flow separation in a rotating annulus with bottom topography. *J. Fluid Mech.* **66**, 303.
- WALKER, J. D. A. & STEWARTSON, K. 1972 The flow past a circular cylinder in a rotating frame. *Z. angew. Math. Phys.* **23**, 745.
- WALKER, J. D. A. & STEWARTSON, K. 1974 Separation and the Taylor-column problem for a hemisphere. *J. Fluid Mech.* **66**, 767.
- WHITE, W. B. 1971 A Rossby wake due to an island in an eastward current. *J. Phys. Oceanogr.* **1**, 161.